A PRINCIPAL COMPONENT APPROACH TO STRUCTURE FORMATION WITH MASSIVE NEUTRINOS

by

Hasmik Hayrapetyan

BSc., Yerevan State University, 2007

THESIS SUBMITTED IN PARTIAL FULFILLMENT

OF THE REQUIREMENTS FOR THE DEGREE OF

MASTER OF SCIENCE

IN THE DEPARTMENT

OF

PHYSICS

SIMON FRASER UNIVERSITY

Spring 2011

APPROVAL

Name:	Hasmik Hayrapetyan
Degree:	Master of Science
Title of thesis:	A Principal Component Approach to Structure Formation with Massive Neutrinos
Examining Committee:	Dr. Jeffrey McGuirk, Chair Assistant Professor, Department of Physics, SFU
	Dr. Levon Pogosian, Senior supervisor Assistant Professor, Department of Physics, SFU
	Dr. Andrei Frolov, Supervisor Assistant Professor, Department of Physics, SFU
	Dr. Howard Trottier, Supervisor Professor, Department of Physics, SFU
	Dr. Dugan O'Neil, Internal Examiner Associate Professor, Department of Physics, SFU
Date Approved:	April 7, 2011

Declaration of
Partial Copyright Licence

Abstract

It will soon become possible to study the evolution of large scale structures with tomographic weak lensing surveys, such as DES and LSST. This will provide a powerful way of constraining the current cosmological model, LCDM, which assumes that neutrinos have zero mass. On linear scales, any small departure of the growth dynamics from the LCDM prediction can be described in terms of two functions of time and scale. Zhao et al derived the principal components of these two functions that will be best constrained by DES and LSST. This thesis demonstrates the possibility of using these principal components to derive the expected constraints on the neutrino mass. It also discusses the effects of neutrino mass on the evolution of cosmological perturbations, and their effect on observables, such as the matter density contrast and the CMB spectrum.

Acknowledgments

I am thankful to Alireza Hojjati for collaboration and Gong-Bo Zhao for providing the principal components.

Contents

List of Figures

Chapter 1

Introduction

1.1 Overview

The standard Lambda Cold Dark Matter (ΛCDM) cosmological model is based on General Relativity (GR). It assumes that universe is filled with baryonic matter, radiation, dark matter and dark energy, represented by a cosmological constant Λ. The existence of dark energy explains the accelerated expansion of the universe, as opposed to gravitational attraction cause by normal matter. This universe also includes massless neutrinos.

According to the inflationary model of cosmology, the early universe was flat, isotropic and homogeneous, but with small fluctuations. As the universe expands, these fluctuations evolve. They are still very small when the universe is dominated by radiation. But at some point, the expansion of the universe becomes dominated by matter, most of which is dark matter that interacts only through gravity. The gravitational forces make the initially small metric and energy-momentum perturbations grow. Those eventually become responsible for large scale structures we see today in the universe.

The theory of GR works very well in our solar system, however the unknown nature of dark matter and dark energy raises doubts about its validity on large scales. Models of modified gravity have been suggested, and ways to test them against observations are being developed. As far as the linear perturbations are concerned, any change in their evolution due to modified gravity can be represented as a modification of the Newton's gravitational constant, and a modified relation between the Newtonian potential and the curvature perturbation.

On the other hand, the evolution of perturbations would also be modified if neutrinos were massive. As neutrinos can only have very small masses, they free stream out of small gravitational potentials and lead to a suppression of growth of structure on small scales as compared to ΛCDM with massless neutrinos.

Future surveys like Dark Energy Survey (DES) and Large Synoptic Survey Telescope (LSST) will provide a way to study the evolution of cosmic structures at several redshifts, using galaxy counts, gravitational weak lensing and Type Ia Supernovae. This will allow for tests of GR on large scales. In [1] it was shown that any departure from ΛCDM growth in linear regime can be encoded into two functions: μ and γ. They equal to unity in ΛCDM but can depend on time and scale in other models. If one could measure these functions with observations, then any specific model that predicts modification of linear growth could be constrained from these functions.

Zhao et al [1] have examined the prospects of measuring functions μ and γ with DES and LSST in combination with CMB data from Planck. In particular, they found the so-called principal components of these two functions, i.e. their uncorrelated degrees of freedom that can be best constrained by the surveys.

In this thesis, we demonstrate that the information stored in the principal components of μ and γ calculated in [1] can be used to forecast the uncertainty in the measurement of the neutrino masser by LSST. Our results are in good agreement with existing forecasts, which were obtained by directly modelling the output of LSST. Methods like this can significantly simplify the process of error forecasts for various models of modified gravity. Rather than calculating the weak lensing, and galaxy count spectra and their cross-correlations for each model, it is sufficient to evaluate the model predictions for functions μ and γ. We expect such methods will be of use to the cosmological community. In addition to these novel results, the thesis examines in detail the effects of the neutrino mass on the evolution of cosmological perturbations.

1.2 Evidence for neutrino mass

In 1930 Pauli has suggested the existence of neutrinos in order to satisfy the energy, momentum and angular momentum conservation in beta-decay. In 1968 neutrinos coming from the sky were detected and observed in laboratory by Homestake experiment [2]. In

1994 LEP experiments [3] have shown that there are three flavours of light neutrinos: electron ν_e, muon ν_μ, and tau ν_τ. These are electrically neutral particles which have half spin and interact through the weak force. In addition, massive neutrinos interact through gravity.

For a long time the Standard Model (SM) of particle physics assumed that neutrinos are massless. However, the Super-Kamiokande [4] and SNO experiments [5] in 2000 have shown that the flavours of neutrinos oscillate. This is a quantum mechanical effect. Neutrinos produced as a certain type end up in a linear combination of three neutrinos after traveling some distance. This can happen only if neutrinos are massive and their masses are different. Neutrinos produced in weak interactions are either an electron neutrino, a muon neutrino, or a tau neutrino. But these different flavours of neutrinos do not have a definite mass. Instead they are composed of two or three slightly different mass states, which can be considered as waves with different frequencies. While the neutrino travels, these three waves interact with each other. There will be points were the frequency of the combined wave is very close to that of the first wave, but at some other point it will be close to the other. This process repeats itself periodically with a frequency defined by the difference of the two wave frequencies. For a matter particle, in this case neutrinos, it is the difference of mass square. This is the reason that neutrino oscillation experiments are sensitive to the difference of the neutrino mass squares, not the absolute value:

$$\Delta m^2_{21} = m^2_2 - m^2_1 \tag{1.1}$$

$$\Delta m^2_{31} = m^2_3 - m^2_1 \tag{1.2}$$

For the mass differences, the neutrino oscillation experiments currently give [6]

$$(\Delta m^2_{21})^{1/2} \simeq 0.009^{+0.0004}_{-0.0006} eV \tag{1.3}$$

$$(\Delta m^2_{31})^{1/2} \simeq 0.047^{+0.010}_{-0.010} eV \tag{1.4}$$

These results provide evidence that at least two flavours of neutrinos are massive.

Experiments aiming to directly measure the neutrino mass have been conducted or being proposed. As mentioned above, neutrinos are produced in β-decay, where a neutron decays into proton, electron/positron and a neutrino/anti-neutrino. The Karlsruhe Tritium Neutrino experiment (KATRIN) [7] is a future experiment that was proposed in order to

measure the endpoint region of the energy spectrum of the tritium beta-decay. They expect to be able to put an upper bound on neutrino mass of

$$m(\nu_e) < 0.35\ eV \tag{1.5}$$

at 95% confidence level.

In addition, a neutrinoless double β-decay has been used, where a neutrino is produced in the first β-decay and it is absorbed in the next β-decay as an antineutrino. Current upper bound on neutrino mass from double β-decay experiments [8] is

$$m(\nu_e) \lesssim 0.9\ eV\ . \tag{1.6}$$

Future double decay experiments are expected to reduce the sensitivity to [6]

$$m(\nu_e) \lesssim 0.05\ eV\ . \tag{1.7}$$

1.3 The dark matter problem

Historically, some additional motivation for massive neutrinos was provided by the dark matter problem in cosmology. The problem occurs when different methods are used to estimate the total amount of matter in the universe. One way to do it is by looking at the amount of luminous matter. Locally, we know the distribution of luminous matter in our galaxy, which will allow us to estimate its mass. Another method is to observe the motion of stars in it. However, the results show that this mass is much larger than the one derived from the luminosity of objects. This was explained by the existence of a new type of matter, dark matter, which was affecting the motion of galaxies. It does not interact with the normal matter via electromagnetic forces.

According to the latest observations of cosmic microwave background (CMB) and surveys of large scale structure, dark matter is 23% of the total matter in the observable universe, while the ordinary matter makes only 4.6%. Ordinary matter includes galaxies, clusters and the other matter that we can observe. Among the candidates of dark matter are MACHOs (Massive Astrophysical Compact Halo Objects) and WIMPs (Weakly Interacting Massive Particles). MACHOs consist of big structures, made of baryonic matter, which almost does not interact with the ordinary matter. They could be made of brown dwarf stars

and black holes. Brown dwarf stars were found near the halo of our galaxy with Hubble telescope. But they make only 6% of galactic halo matter. This means that there are also other forms of dark matter near the halo. WIMPs, which consist of subatomic particles, are thought to be made of non-baryonic matter.

Neutrinos, being weakly interacting particles, have also been considered as dark matter candidates. This would be what is known as hot dark matter (HDM), so called for the relativistic speed of the particles. It is now clear that HDM cannot be the only component of dark matter in the universe. They cannot explain the structure formation on small scales, because they move fast, erasing all the structures on this scales. If they made the dark matter, large scale structures would form first, and then small, which is called a "top-down" scenario. This contradicts the observational data, which show that galaxies are older than clusters. Thus cosmology provides a lower limit on the fraction of dark matter in neutrinos. The fraction of energy density in neutrinos is given by

$$\Omega_\nu = \frac{\sum_i m_i}{93.14 h^2 eV} , \tag{1.8}$$

which will be discussed in next chapter. According to the WMAP 7 data, the upper bound on the sum of the neutrino masses is $0.58eV$ [9]. This implies that light neutrinos with $0.5eV$ masses will roughly make only one tenth of dark matter, and thus other dark matter components should be considered too.

Massive (sterile) neutrinos can also make the dark matter, which in this case will be called warm dark matter (WDM). But there are some limitations on their masses. Tremaine and Gunn [10] assumed that the dark matter in galactic halos are made of neutrinos. They have shown that for this to be true, their mass should satisfy

$$m_\nu \geqslant 1MeV . \tag{1.9}$$

It is likely that neutrinos need to have much bigger masses in order to be cold dark matter. We should mention two things here. First, the cross section of neutrino annihilation depends on their mass: neutrinos with small masses ($m_\nu < 1MeV$) would have small annihilation cross section. On the other hand, these neutrinos would decouple from the rest of the plasma earlier than heavy neutrinos. This will result in increased neutrino abundance at the time of neutrino decoupling, which will make the present number of neutrinos really big. Correspondingly, the energy density in the neutrinos would be much bigger. In order

for these light neutrinos not to result in a spatially closed universe, there should be a lower bound on their mass. Based on this argument, B. Lee and S. Weinberg [11] have shown that in order for heavy massive neutrinos to form the dark matter, their mass should be

$$m_\nu \geqslant 2GeV. \tag{1.10}$$

1.4 Fisher information matrix

Fisher information matrix can be used to predict the ability of future observations to constrain cosmological parameters from a set of expected observables. Let's assume we have observables y_b, $b \in \{1,....B\}$, where each of them has Gaussian uncertainty σ_b. We will assume that different y_b observables are uncorrelated. Suppose also that there is a theoretical model that can predict their values using a function f_b that depends on some model parameters p. We can then write the Fisher matrix which predicts the information one can get about a parameter from y_b. The likelihood of observing a particular set of observable y_b within a given model is

$$P(y|p) \propto \exp\left(-\frac{1}{2}\chi^2\right), \tag{1.11}$$

where

$$\chi^2 = \sum_{b=1}^{B} \frac{(f_b(p)-y_b)^2}{{\sigma_b}^2}\,. \tag{1.12}$$

According to Bayes theorem

$$P(p|y) = \frac{P(y|p)P(p)}{P(y)}\,, \tag{1.13}$$

namely, the likelihood of a set of parameters given the observables is proportional to the likelihood of observables given the parameters. In the above, $P(p)$ is the prior probability of parameters. In the absence of theoretical prediction, it is common to take it to be constant over a fixed range. We will state what we assumed for the priors where applicable. Suppose the true value of a parameter is p_0, i.e this is the value at peak of the likelihood. We can expand the likelihood at the point $p^i = p^i_0 + \delta p^i$ near the the peak. The expansion of the χ^2 is

$$\langle\chi^2(p)\rangle = \langle\chi^2\rangle + \langle\frac{\partial\chi^2}{\partial p^j}\rangle\delta p^j + \frac{1}{2}\langle\frac{\partial^2\chi^2}{\partial p^j\partial p^k}\rangle\delta p^j\delta p^k + ... \tag{1.14}$$

Here expectation values are taken at the true value p_0. The first term is zero. The second term will also vanish, as $f_b(p_0) = y_b$. In the expansion of $\exp\left(\chi^2\right)$ the lowest order non-zero term is

$$\exp\left(-\frac{1}{2}\chi^2\right) = \exp\left(-\frac{1}{4}\langle\frac{\partial^2\chi^2}{\partial p^j \partial p^k}\rangle \delta p^j \delta p^k\right) = \exp\left(-\frac{1}{2}F_{jk}\delta p^j \delta p^k\right) , \tag{1.15}$$

where F_{jk} is the Fisher matrix:

$$F_{jk} = \sum_b \frac{1}{\sigma_b^2}\frac{\partial f_b}{\partial p^j}\frac{\partial f_b}{\partial p^k} . \tag{1.16}$$

The covariance matrix is defined as

$$C_{jk} = \langle \delta p_j \delta p_k \rangle = \left(F^{-1}\right)^{jk} . \tag{1.17}$$

Marginalized errors of the parameters are given by $\sigma(p_i) = \sqrt{(F^{-1})_{ii}}$. More generally, we can find the components of Fisher matrix, if we know the likelihood $P(p^i|y_b)$ of the parameters with given observables.

1.5 Principal component analysis

Errors on model parameters derived from a particular set of observables will in general be correlated. Principal component analysis (PCA) is a way to find a new set of uncorrelated parameters which are linear combinations of the original ones.

Lets assume that we have a set observables y_b, which gives us some information about a function $q(x)$. This function can be discretized on x as

$$q(x) - q_0 = \sum_{i=1}^{N} q_i s_i(x) \tag{1.18}$$

where $x_1 < x_2 < ... < x_{i-1} < x_i < ...x_N$ and $s_i = 1$ if $x_i < x < x_{i+1}$, otherwise $s_i = 0$. In this case we think of quantities q_i as a set of model parameters. Assume, there is a theoretical prediction for this dependence. We also know what the observational results would be. Our aim is to find how well these parameters can be constrained by data. For this case, the Fisher matrix is

$$F_{ij} = \sum_b \frac{1}{\sigma_{y,b}^2}\frac{\partial y_b}{\partial q^i}\frac{\partial y_b}{\partial q^j} = C_{ij}^{-1} , \tag{1.19}$$

where $C_{ij} = \langle (q_i - \bar{q}_i)(q_j - \bar{q}_j) \rangle$ is the covariance matrix. The covariance matrix is diagonal only if parameters q_i are uncorrelated. In general, the uncertainties of different q_i are correlated too and the covariance is non-diagonal. Also, if we increase the number of the points N at which we discretized our function, the number of parameters will increase and the effect of a particular q_i on the observables will be negligible, i.e. any of the terms $\partial y_b / \partial q_i$ will be very small. As a result, covariance, which is the inverse of Fisher matrix, will generally be very large. Since

$$C_{ii} = F_{ii}^{-1} = \sigma^2(q_i) \tag{1.20}$$

many more parameters will lead to bigger uncertainties.

PCA is a way to converge to a small number of well-constrained uncorrelated parameters that a given data set can measure. For this we should diagonalize the covariance matrix. Since C_{ij} is a symmetric matrix, it is possible to diagonalize it with its own eigenvectors. Let $W_{ij} = e_i(z_j)$ be its orthonormal eigenvectors, such that

$$\int e_i(x_k) e_j(x_k) dx_k = \delta_{ij} \ . \tag{1.21}$$

Then the diagonalized covariance matrix can be found from

$$C = W^T \Lambda W, \tag{1.22}$$

where $\Lambda_{ij} = \lambda_i \delta_{ij}$ is a diagonal matrix. One can write parameter q_i as an expansion in this basis:

$$q_i = \sum_j e_j(x_i) \alpha_j \ , \tag{1.23}$$

where p_i is the new parameter. From (1.23) it follows that

$$\alpha_i = \int e_i(x_j) q_j dx_j \ . \tag{1.24}$$

The new covariance matrix

$$\Lambda_{ij} = \langle (\alpha_i - \bar{\alpha}_i)(\alpha_j - \bar{\alpha}_j) \rangle = \lambda_i \delta_{ij} \tag{1.25}$$

is uncorrelated and $\lambda_i = \sigma^2(\alpha_i)$. From (1.24) we obtain

$$q_i = q(x_i) - q_0 = \sum_j e_j(x_i) \alpha_j \ . \tag{1.26}$$

In the limit of $N \to \infty$, the last equation can be written as

$$q(x) - q_0 = \sum_j e_j(x) \alpha_j \ . \tag{1.27}$$

1.6 Storing and retrieving information using PCA

Suppose now that we have a particular functional form of $q(x)$, which depends on a couple of parameters a and b. For example, we could have $q(x) = a + bx$. As it turns out, one can find the uncertainties in parameters a and b given the eignenvalues and eigenmodes $\{e_j(x), \lambda_j\}$ of $q(x)$ obtained in the previous section. Namely, the Fisher matrix for a and b can be written as

$$F_{ab} = \sum_{ij} \frac{\partial q_i}{\partial p^a} \frac{1}{C_{ij}} \frac{\partial q_j}{\partial p^b} \ . \tag{1.28}$$

One can interpret the above equations as treating the measured values of q_i as a set of observables, instead of the original set y_b. We can then expand $\partial q(x)/\partial p^a$ in the new basis:

$$\frac{\partial q(x)}{\partial p^a} = \sum_j \alpha_j^{(a)} e_j(x) \ , \tag{1.29}$$

and substitute into Eq. (1.28), giving us

$$F_{ab} = \sum_k \alpha_k^{(a)} \alpha_k^{(b)} \lambda_k^{-1} \ . \tag{1.30}$$

Thus, PCA of $q(x)$ can be thought of as a way of storing information about $q(x)$ in a way that is independent of a particular functional form. If one wants to constrain parameters of any particular form of $q(x)$, it can be done from the existing eigenmodes. Another advantage of this approach is data compression. Namely, in practice, only a small number of eigenmodes have small errors (i.e. small eigenvalues), and only the few best constrained modes need to be included in the sum. We will demonstrate this in Chapter 6.

Chapter 2

Neutrinos in Cosmology

2.1 Neutrino decoupling temperature

The standard Big Bang theory predicts a large number of neutrinos per flavour in the visible universe. These neutrinos were produced at high temperatures by weak interactions. In the early universe, because of cosmic weak interactions, they were in thermal equilibrium with the rest of plasma. As the universe expanded, this interaction rate decreased. At some point it was equal to the expansion rate H of the universe. This is when neutrinos decoupled from the rest of plasma. We can estimate the temperature of neutrino decoupling by comparing these two rates. The interaction rate is

$$\Gamma_\nu \propto \sigma_\nu \cdot n_\nu \ , \tag{2.1}$$

where n_ν is the neutrino number density,

$$n_\nu \propto T^3 \ , \tag{2.2}$$

and σ_ν is the $e - \nu_e$ interaction cross section:

$$\sigma_\nu \propto G_F^2 \cdot T^2 \ , \tag{2.3}$$

where G_F is Fermi coupling constant. Therefore, we get

$$\Gamma_\nu \propto T^5 \cdot G_F^2 \ . \tag{2.4}$$

The expansion rate is given by

$$H = \sqrt{\frac{8\pi G\rho}{3}}\ , \tag{2.5}$$

where G is the gravitational constant and ρ is the density. Neutrinos decoupled during the radiation dominated era of the universe, for which the density $\rho \propto T^4$. Setting Γ_ν equal to H, and substituting the radiation density in the expression for H, gives us the decoupling temperature

$$T_{dec} \approx \left[\frac{\sqrt{G}}{G_F^2}\right]^{1/3} \approx 1MeV\ . \tag{2.6}$$

2.2 Temperature of neutrinos today

When the temperature of the universe reached 1 MeV, neutrinos decoupled from the rest of the plasma. However, for some time neutrinos and photons continued to have the same temperature evolution. At some point, the temperature of the universe fell below the electron mass, which allowed electrons and positrons to annihilate. Because the neutrinos were already decoupled, the energy density and entropy of electrons and positrons are transferred to the photons, but not to neutrinos. After this time, the temperature of neutrinos has been different from that of the rest of the plasma.

It is possible to calculate the temperature of neutrinos today by writing the entropy density of the universe before and after the electron-positron annihilation. According to the second law of thermodynamics, the entropy of the universe can only increase or stay the same. But the entropy produced by different processes is small compared to the total entropy of the universe. Therefore, we can safely ignore all the changes and approximate the expansion of the universe as an adiabatic process. For each spin state entropy density for massless bosons is $2\pi T^3/45$. For massive fermions it is $7/8$ of that. Before annihilation the only bosons are photons with 2 spin states, while the relevant fermions are the electrons and positrons, with 2 spin states each. This shows that before annihilation, when the temperature of the universe and decoupled neutrinos is T_1, the entropy density is

$$s(a_1) = \frac{2\pi^2}{45}{T_1}^3[2+(7/8)(2+2)] \tag{2.7}$$

After annihilation, the entropy density is

$$s(a_2) = \frac{2\pi^2}{45} 2T_\gamma{}^3 \tag{2.8}$$

As the entropy density is conserved, the ratio of temperatures is

$$\frac{T_\nu}{T_\gamma} = \left(\frac{4}{11}\right)^{1/3}, \tag{2.9}$$

resulting in $T_\nu = 1.95K$ today if we use $T = 2.726$K for the current temperature of CMB photons.

2.3 Distribution of neutrinos in the universe

While coupled to the plasma, neutrinos satisfy the equilibrium Fermi-Dirac distribution

$$f_{eq}(p) = \left[\exp\left(\frac{p-\mu_\nu}{T}\right) + 1\right]^{-1}, \tag{2.10}$$

where μ_ν is the neutrino chemical potential. Before the time of Big Bang Nucleosynthesis (BBN), because of neutrino oscillations, their flavours were in equilibrium. In [12] it was shown that all the flavours share the same small value of chemical potential. Therefore, the chemical potential can be safely ignored.

In the standard cosmological model, the neutrino decoupling is approximated with an instantaneous process [13]. After the decoupling, the distribution function $f_{eq}(p)$ stays the same, while the temperature and the momentum of neutrinos decrease as a^{-1} with the expansion of the universe. This means that in comoving coordinates the number density of neutrinos will remain the same after the decoupling. Using the neutrino momentum distribution function, we can estimate the neutrino number density per flavour as

$$n_\nu = \int \frac{f_{eq}(p)}{(2\pi)^3} d^3p = \frac{3}{11} n_\gamma = \frac{6\zeta(3)}{11\pi^2} T_\gamma^3 \tag{2.11}$$

where $\zeta = 1.202$ is the Riemann's zeta function [14], and T_γ is the photon temperature at a given time. From this equation we can find the number of neutrinos and antineutrinos of each flavor per cm^3 today, which is approximately 113.

For relativistic neutrinos the energy density for one neutrino flavour can be calculated from the distribution function as

$$\rho_\nu(m_\nu \ll T_\nu) = \frac{7\pi^2}{120}\left(\frac{4}{11}\right)^{4/3} T_\gamma^4 \,. \tag{2.12}$$

After the neutrino decoupling, but before becoming non-relativistic (i.e. while $m_\nu \ll T_\nu$), neutrinos contribute to the radiation energy density of the universe

$$\rho_R = \rho_\gamma + \rho_\nu = \left[1 + \frac{7}{8}\left(\frac{4}{11}\right)^{4/1} N_{eff}\right]\rho_\gamma \tag{2.13}$$

where

$$\rho_\gamma = \frac{2\pi^2}{30} T_\gamma^4 \tag{2.14}$$

is the photon energy density, and N_{eff} is the effective number of relativistic neutrinos. In the standard model there are no other relativistic particles and $N_{eff} = 3.046$ [6]. It is not exactly equal to 3 because the neutrinos were somewhat heated by the electron-positron annihilation processes, as the neutrino decoupling was not completely over before that annihilation started. Any deviation from this number would imply existence of other relativistic particles in addition to the three flavours of neutrinos and photons. There are some constrains on N_{eff} coming from cosmology. The BBN analysis is consistent with a range of $1.90 < N_{eff} < 3.77$, while the WMAP three year data implies $N_{eff} = 3.3^{+0.9}_{-4.4}$.

If the neutrinos were massive and non-relativistic, their energy density would be

$$\rho_\nu(m_\nu \gg T_\nu) = m_\nu n_\nu. \tag{2.15}$$

After becoming non-relativistic the contribution of massive neutrinos to the energy density in the universe is

$$\Omega_\nu = \frac{\rho_\nu}{\rho_c} = \frac{\sum_i m_i}{93.14 h^2 eV} \tag{2.16}$$

where we used (2.15), neutrino number density $n_\nu = 112 cm^{-3}$ and critical energy density of the universe today $\rho_c = 1.8788 * 10^{-29} h^2 g cm^{-3}$. Here $\sum_i m_i = 3m_0$ if the three neutrinos have the same mass m_0, h is the present Hubble parameter in $100 kms^{-1} Mpc^{-1}$ units. The above equation is valid for non-degenerate neutrinos as well. From this equation it is possible to obtain a rough estimate of the neutrino mass. If we assume three degenerate neutrinos with masses $m_0 = \sum_i m_i/3$, and also consider the fact that neutrino density portion Ω_ν is much smaller than $\Omega_M \simeq 0.3$, we obtain $m_0 \lesssim 5eV$.

2.4 The neutrino free streaming length

The effect of the neutrino free streaming length is similar to that of the Jean's length, and we find it helpful to review it first (although its physical origin is different). When particles of a gas are far enough from each other, they attract due to gravity. But as they get very close to each other, below a certain distance, there will be a repulsive force (electromagnetic in nature) preventing the gas from collapsing. The length scale below which the gas does not collapse is called the Jean's length. The Jean's wavenumber and the Jean's length [6] are defined as

$$k_J(t) = \left(\frac{4\pi G\bar{\rho}(t)a^2(t)}{{c_s}^2(t)}\right)^{1/2} \tag{2.17}$$

$$\lambda_J(t) = 2\pi\frac{a(t)}{k_J(t)} = 2\pi\sqrt{\frac{2}{3}}\frac{c_s(t)}{H(t)} \tag{2.18}$$

where c_s is the sound speed, H(t) is the Hubble constant, and $\bar{\rho}(t)$ is the average gas density.

It is possible to define the neutrino free streaming length in a similar way. Because they can stream out of small scale gravitational potentials, neutrinos do not collapse on scales smaller than a particular length scale λ_{FS}. This is essentially the maximum distance that neutrinos can travel freely. On scales larger than λ_{FS}, gravitational potentials are big and neutrinos can not escape them, and so they cluster. On smaller scales gravitational potentials are smaller than the kinetic energy of neutrinos. The thermal velocity v_{th} here plays the role of resistance, similar to the way in which electromagnetically induced pressure plays the role of the resistance for the Jean's length. Thus, we can define the free-streaming wavenumber and wavelength in the same way as we did for the Jean's length by replacing the sound speed with the thermal velocity of neutrinos:

$$k_{FS}(t) = \left(\frac{4\pi G\bar{\rho}(t)a^2(t)}{{v_{th}}^2(t)}\right)^{1/2} \tag{2.19}$$

$$\lambda_{FS}(t) = 2\pi\frac{a(t)}{k_{FS}(t)} = 2\pi\sqrt{\frac{2}{3}}\frac{v_{th}(t)}{H(t)} \tag{2.20}$$

As massless neutrinos travel with the speed of light, their free streaming length equals to the Hubble radius. For massive neutrinos, on the other hand, we have

$$v_{th} = \frac{\langle p\rangle}{m} \simeq \frac{3T_\nu}{m} = \frac{3T_\nu^0}{m}\left(\frac{a_0}{a}\right) \simeq 150(1+z)\left(\frac{1eV}{m}\right) km/s\,, \tag{2.21}$$

where T_ν^0 is the neutrino temperature today. During the matter or Λ dominated eras, Eqs. (2.19)-(2.21) give

$$\lambda_{FS}(t) = 7.7 \frac{1+z}{\sqrt{\Omega_\Lambda + \Omega_M (1+z)^3}} \left(\frac{1eV}{m}\right) h^{-1} Mpc \tag{2.22}$$

$$k_{FS}(t) = 0.82 \frac{\sqrt{\Omega_\Lambda + \Omega_M (1+z)^3}}{(1+z)^2} \left(\frac{m}{1eV}\right) h/Mpc \ , \tag{2.23}$$

where Ω_Λ and Ω_M are the cosmological constant and matter density fractions today.

2.5 The non-relativistic transition for massive neutrinos

The energy of a neutrino can be written as $\varepsilon^2 = q^2 + a^2 m^2$, where m is its mass, a is the scale factor and q is the comoving momentum. At the time of neutrino decoupling, a is very small, which means that rest energy am is very small compared to the kinetic energy q^2. As a grows, the term am increases. Starting from some value of a, the rest mass cannot be ignored. This marks the transition of neutrinos from relativistic to non-relativistic, and it happens when $p_\nu \sim m_\nu$, or, equivalently, $T_{\nu nr} = m_\nu/3$. The corresponding redshift is

$$1 + z_{nr} = \frac{T_{\nu,nr}}{T_{\nu 0}} = 1.99 \times 10^3 (m_\nu/eV) \tag{2.24}$$

The redshift of the radiation-matter equality is $z_{eq} \sim 3000$, and thus for sub-eV neutrino masses that are of interest to cosmology, the transition happens during the matter-domination epoch.

Chapter 3

Cosmological Perturbations

3.1 Background evolution

In the standard Big Bang model the universe is assumed to be homogeneous on very large scales, and is described by the Friedmann-Robertson-Walker (FRW) metric [15]

$$ds^2 = \bar{g}_{\mu\nu} dx^\mu dx^\nu = a^2(\tau)[-d\tau^2 + \delta_{ij} dx^i dx^j] \,, \tag{3.1}$$

where a is the scale factor and τ is the conformal time related to the proper time t through $ad\tau = dt$. In what follows we will take $\hbar = c = 1$. For a homogeneous FRW universe, the Einstein equations give

$$\left(\frac{\dot{a}}{a}\right)^2 = \frac{8\pi}{3} G a^2 \bar{\rho} - k \tag{3.2}$$

$$\frac{d}{d\tau}\left(\frac{\dot{a}}{a}\right) = -\frac{4\pi}{3} G a^2 (\bar{\rho} + 3\bar{P}) \tag{3.3}$$

where $\bar{\rho}$ is the energy density, $\bar{P}$ is the pressure, and the dot means a derivative with respect to τ. CMB measurements by BOOMERANG [16] and MAXIMA [17] in 2000, and later by WMAP [18], strongly favour a universe which is almost spatially flat, which means we can set $k = 0$. With this, the background evolution of the Universe is described by

$$H^2 = \frac{8\pi G}{3}(\rho_\gamma + \rho_{cdm} + \rho_b + \rho_\nu + \rho_\Lambda) \tag{3.4}$$

where H is the Hubble parameter, defined as $H = d(\ln a)/dt = \dot{a}/a^2$, the dot again denotes a derivative with respect to the conformal time τ, and ρ_γ, ρ_{cdm}, ρ_b, ρ_ν, ρ_Λ are respectively

the homogenous densities of photons, cold dark matter (CDM), baryons, neutrinos and dark energy. The density of photons and massless neutrinos decrease as a^{-4}, while CDM, baryons and massive neutrinos decrease as a^{-3}. We assume that the dark energy is the cosmological constant, also favoured by current observations, and is time-independent. In the radiation dominated era, the scale factor is $a \propto \tau$, while in the matter dominated era we have $a \propto \tau^2$.

3.2 Cosmological perturbations

The homogeneous universe is a good approximation on largest scales, but it cannot describe the matter distribution in the universe and explain the structure formation. Let us consider a universe with small departures from homogeneity. We can write the metric ($g_{\mu\nu}$) and energy-momentum ($T_{\mu\nu}$) as their background value plus perturbations:

$$g_{\mu\nu}(\vec{x},t) = \bar{g}_{\mu\nu}(t) + h_{\mu\nu}(\vec{x},t) \tag{3.5}$$

$$T_{\mu\nu}(\vec{x},t) = \bar{T}_{\mu\nu}(t) + \delta T_{\mu\nu}(\vec{x},t) \tag{3.6}$$

During the radiation domination the growth of matter perturbations is suppressed. After the onset of matter domination, perturbations in CDM begin to grow due to gravitational attraction, while those of baryons and photons do not because of their tight electromagnetic coupling. But after the decoupling of photons and baryons, perturbations of the baryon density begin to grow as well and eventually catch up with those of CDM. Eventually, perturbations in matter density become larger than the background density.

In this thesis only linear perturbations, which describe the universe at early times and/or large scales, will be discussed. We will assume adiabatic initial conditions for the perturbations, favoured by simplest models of Inflation, where one takes initial fractional perturbations in all matter components to be equal. Working to linear order in perturbations results in separate equations for each Fourier mode. This will be discussed later in this chapter.

3.3 Linear perturbation theory

In the longitudinal Newtonian gauge, the line element in the presence of metric perturbations is given by

$$ds^2 = g_{\mu\nu}dx^\mu dx^\nu = a^2(\tau)[-(1+2\psi)d\tau^2 + (1-2\phi)\delta_{ij}dx^i dx^j] \tag{3.7}$$

where perturbations are described by scalar potentials ϕ and ψ. It is obvious that there are no vector and tensor perturbations in this gauge: we have only scalar diagonal perturbations. Metric and energy-momentum perturbations are related to each other through the Einstein equation. Different components of the perturbed Einstein equation in Fourier space give us

$$3\left(\frac{\dot{a}}{a}\right)^2\psi + 3\frac{\dot{a}}{a}\dot{\phi} + k^2\phi = 4\pi G a^2 \delta T^0{}_0 \tag{3.8a}$$

$$k^2\left(\frac{\dot{a}}{a}\psi + \dot{\phi}\right) = 4\pi G a^2(\bar{\rho}+\bar{P})\theta \tag{3.8b}$$

$$\left(2\frac{\ddot{a}}{a} - \left(\frac{\dot{a}}{a}\right)^2\right)\psi + \frac{\dot{a}}{a}(\dot{\psi}+2\dot{\phi}) + \ddot{\psi} + \frac{k^2}{3}(\phi-\psi) = 4\pi G a^2 \delta T^i{}_i \tag{3.8c}$$

$$k^2(\phi-\psi) = 12\pi G a^2(\bar{\rho}+\bar{P})\sigma \tag{3.8d}$$

where $\theta = ik^j v_j$ and σ are, respectively, the divergence of the fluid velocity and the shear, related to the energy-momentum tensor via

$$(\bar{\rho}+\bar{P})\,\theta = ik^j \delta T^0{}_j \tag{3.9}$$

$$(\bar{\rho}+\bar{P})\,\sigma = -\,(\hat{k}_i\hat{k}_j - \frac{1}{3}\delta_{ij})\Sigma^i_j\ , \tag{3.10}$$

where

$$\Sigma^i{}_j = T^i{}_j - T^k{}_k\delta^i{}_j \tag{3.11}$$

is the traceless part of energy-momentum tensor $T^i{}_j$ and k is the comoving wave number. If we assume that the universe is filled with perfect fluid, then the energy-momentum tensor is given by

$$T^\mu{}_\nu = P g^\mu{}_\nu + (\rho+P)U^\mu U_\nu \tag{3.12}$$

where U^μ is the four velocity of the fluid, and P and ρ are the pressure and density of the fluid measured by the comoving observer, who is at rest with respect to the fluid. If the

velocity of the fluid is very small, then we can consider it as a first order perturbation. For the energy momentum tensor we will have

$$T^0{}_0 = -(\bar{\rho} + \delta\rho) \tag{3.13}$$

$$T^0{}_i = (\bar{\rho} + \bar{P})v_i = -T^i{}_0 \tag{3.14}$$

$$T^i{}_i = (\bar{P} + \delta P)\delta^i{}_j + \Sigma^i{}_j \tag{3.15}$$

$$\Sigma^i{}_i = 0 \tag{3.16}$$

From the covariant conservation of energy-momentum, we can derive the continuity equation

$$\dot{\delta} = -(1+\omega)(\theta - 3\dot{\phi}), \tag{3.17}$$

and the Euler equation

$$\dot{\theta} = -\frac{\dot{a}}{a}(1-3\omega)\theta - \frac{\dot{\omega}}{1+\omega}\theta + \frac{\omega}{1+\omega}k^2\delta - k^2\sigma + k^2\psi, \tag{3.18}$$

where $\omega = P/\rho$ is the equation of state. These equations can be used both for individual components and for the whole fluid. From (3.8a) and (3.8b) we can get the Poisson equation

$$k^2\psi_k = 4\pi G a^2 \delta\rho = 4\pi G a^2 \rho \Delta_k \tag{3.19}$$

where $\Delta_k = \delta + 3H\theta/k$ is the so-called comoving density contrast, which is a gauge-invariant quantity [6].

3.4 Phase space and the Boltzmann equation

Phase-space is described by three comoving coordinates x^i and the three conjugate momenta P_i. Conjugate momenta are the spatial parts of the 4-momentum $P_i = mU_i$, where $U_i = dx_i/\sqrt{-ds^2}$ is the 4-velocity of the fluid. This momentum is related to the proper momentum p_i measured by an observer with fixed coordinates by

$$P_i = a(1-\phi)p_i \ . \tag{3.20}$$

In other words, p_i is the physical momentum. If there are no metric perturbations, P_i is constant and p_i decreases as a^{-1}. In some cases we can ignore perturbations and replace

the conjugate momentum P_i with a comoving one $q_i = ap_i$, which does not include perturbations. The time-component of the 4-momentum can be written as

$$P_0 = -(1+\psi)\varepsilon \,, \tag{3.21}$$

where ε is defined as the proper energy times the scale factor, $\varepsilon = a(p^2+m^2)^{1/2} = (q^2 + a^2m^2)^{1/2}$, which is the energy measured in comoving coordinates.

The number of particles in the volume $dx^1dx^2dx^3dP_1dP_2dP_3$ is described by the phase-space distribution $f(x^i, P_j, \tau)$:

$$dN = f(x^i, P_j, \tau)dx^1dx^2dx^3dP_1dP_2dP_3 \,. \tag{3.22}$$

If there are no perturbations, then the distribution is

$$f_0 = f_0(\varepsilon) = \frac{1}{e^{\varepsilon/T_0}+1} \tag{3.23}$$

for fermions, and

$$f_0 = f_0(\varepsilon) = \frac{1}{e^{\varepsilon/T_0}-1} \tag{3.24}$$

for bosons, where $T_0 = aT$ is the temperature today. The energy-momentum tensor is related to the phase-space distribution and the 4-momentum P_μ as

$$T_{\mu\nu} = \int dP_1dP_2dP_3(-g)^{-1/2}\frac{P_\mu P_\nu}{P^0}f(x^i, P_j, \tau) \,, \tag{3.25}$$

where $(-g)^{-1/2} = a^{-4}(1-\pi+3\psi)$ is the determinant of $g_{\mu\nu}$. If the perturbations are small, we can write the phase-space distribution as

$$f(x^i, P_j, \tau) = f_0(q)[1+\Psi(x^i, q, n_j, \tau)] \tag{3.26}$$

where Ψ is the perturbation of the distribution.

The comoving 3-momentum can be expressed in terms of its magnitude and direction: $q_j = qn_j$. In that case, the Boltzmann equation for the phase-space distribution is

$$\frac{Df}{d\tau} = \frac{\partial f}{\partial\tau} + \frac{dx^i}{d\tau}\frac{\partial f}{\partial x^i} + \frac{dq}{d\tau}\frac{\partial f}{\partial q} + \frac{dn_i}{d\tau}\frac{\partial f}{\partial n_i} = \left(\frac{\partial f}{\partial\tau}\right)_C \,, \tag{3.27}$$

where the last term describes redistribution of particles due to collisions. We will consider only terms which are first order in perturbations. We note that $dx^i/d\tau = q_i/\varepsilon$ is of zero-th

order, and to the first order, $\partial f/\partial x^i$ is Ψ. From the geodesic equation, $P^0\dot{P}^0+\Gamma^0_{\mu\nu}P^\mu P^\nu=0$, it is easy to show that

$$\frac{dq}{d\tau}=q\dot{\phi}-\varepsilon(q,\tau)n_i d_i\psi\ , \tag{3.28}$$

which is first order in perturbations. df/dn_i contributes at first order. In order to have $(dn_i/d\tau)(df/dn_i)$ term in first order, therefore we should take the zero order of $dn_i/d\tau$, which equals to zero. So the forth term in (3.27) will be zero. Considering all these, the Boltzmann equation in Fourier space can be written as

$$\frac{d\Psi}{d\tau}+i\frac{q}{\varepsilon}(\vec{k},\hat{n})\Psi+\frac{d\ln f_0}{d\ln q}\left[\dot{\phi}-i\frac{\varepsilon}{q}(\vec{k},\hat{n})\psi\right]=\frac{1}{f_0}\left(\frac{df}{d\tau}\right)_C \tag{3.29}$$

For collisionless particles, such as neutrinos after decoupling, or the CDM, the Boltzmann equation is

$$\frac{d\Psi}{d\tau}+i\frac{q}{\varepsilon}(\vec{k},\hat{n})\Psi+\frac{d\ln f_0}{d\ln q}\left[\dot{\phi}-i\frac{\varepsilon}{q}(\vec{k},\hat{n})\psi\right]=0\ , \tag{3.30}$$

which is also called the Vlasov equation. Note that in the Fourier decomposition we will be using comoving wavelengths $(2\pi/k)$, where $\mathbf{k}$ is the comoving wave vector. The physical wavelength is $\lambda=a(t)2\pi/k$.

3.5 Massless neutrinos

We would like to write down the equations for perturbations in a universe with massless neutrinos. Using relations $(-g)^{-1/2}=a^{-4}(1-\psi+3\phi)$ and $dP_1dP_2dP_3=(1-3\phi)q^2dqd\Omega$, given in Newtonian gauge, we can find the components of energy-momentum tensor T^μ_ν:

$$T^0{}_0=-a^{-4}\int q^2dqd\Omega qf_0(q)(1+\Psi) \tag{3.31}$$

$$T^0{}_i=a^{-4}\int q^2dqd\Omega qn_if_0(q)\Psi \tag{3.32}$$

$$T^i{}_j=a^{-4}\int q^2dqd\Omega\frac{q^2n_in_j}{q}f_0(q)(1+\Psi) \tag{3.33}$$

Energy density and pressure are $\rho_\nu=3P_\nu=-T^0{}_0=T^i{}_i$. Equations (3.31) and (3.33) for unperturbed part of energy density and pressure give us

$$\bar{\rho}_\nu=3\bar{P}_\nu=a^{-4}\int q^2dqd\Omega qf_0(q)=4\pi a^{-4}\int q^2dqqf_0(q). \tag{3.34}$$

For perturbed energy density $\delta\rho_\nu$, pressure δP_ν, energy flux $\delta T^0_{\nu i}$ and anisotropic stress $\Sigma^i_{\nu j} = T^i_{\nu i} - P_\nu \delta^i_j$ we will have

$$\delta\rho_\nu = 3\delta P_\nu = a^{-4} \int q^2 dq d\Omega q f_0(q) \Psi \tag{3.35}$$

$$\delta T^0_{\nu i} = a^{-4} \int q^2 dq d\Omega q n_i f_0(q) \Psi \tag{3.36}$$

$$\Sigma^i_{\nu j} = a^{-4} \int q^2 dq d\Omega q \left(n_i n_j - \frac{1}{3}\delta_{ij} \right) f_0(q) \Psi \tag{3.37}$$

As the momentum distribution function for relativistic neutrinos depends only on momentum, it is easily integrable. We can introduce the distribution function of mean momentum by integrating out the q-dependence in the distribution function f_0:

$$F_\nu \left(\vec{k}, \hat{n}, \tau \right) = \frac{\int q^2 dq q f_0(q) \Psi}{\int q^2 dq q f_0(q)} = \sum_{l=0}^{\infty} \left(-i^l \right) (2l+1) F_{\nu l}(\vec{k}, \tau) P_l(\hat{k} \cdot \hat{n}) \ , \tag{3.38}$$

where we further expanded F_ν into a Legendre series. Using this in equations (3.34) and (3.35), we can write the density contrast δ_ν, the velocity gradient θ_ν and the shear σ_ν in terms of the new distribution function as

$$\delta_\nu = \frac{1}{4\pi} \int d\Omega F_\nu \left(\vec{k}, \hat{n}, \tau \right) = F_{\nu 0} \tag{3.39}$$

$$\theta_\nu = \frac{3i}{16\pi} \int d\Omega \left(\vec{k} \cdot \hat{n} \right) F_\nu \left(\vec{k}, \hat{n}, \tau \right) = \frac{3}{4} k F_{\nu 1} \tag{3.40}$$

$$\sigma_\nu = -\frac{3}{16\pi} \int d\Omega \left[\left(\vec{k} \cdot \hat{n} \right)^2 - \frac{1}{3} \right] F_\nu \left(\vec{k}, \hat{n}, \tau \right) = \frac{1}{2} F_{\nu 2} \ , \tag{3.41}$$

where θ and σ were introduced in the beginning of Chapter 3. Using the definition of F_ν in equation (3.30) we obtain

$$\frac{dF_\nu}{d\tau} + ik\mu F_\nu = 4(\dot{\phi} - ik\mu\psi) \ , \tag{3.42}$$

where $\mu = \hat{k} \cdot \hat{n}$. Further, using the Legendre expansion of F_ν, we get the evolution equations for the density contrast, velocity gradient and shear:

$$\dot{\delta}_\nu = -\frac{4}{3}\theta_\nu + 4\dot{\phi}, \tag{3.43}$$

$$\dot{\theta}_\nu = k^2 \left(\frac{1}{4}\delta_\nu - \sigma_\nu \right) + k^2 \psi, \tag{3.44}$$

$$\dot{F}_{\nu l} = \frac{k}{2l+1}\left[lF_{\nu(l-1)} - (l+1)F_{\nu(l+1)}\right], l \geq 2\ . \tag{3.45}$$

Note that (3.43) and (3.44) are the continuity and Euler equations. Combining those two, we can find the equation for the density contrast:

$$\ddot{\delta}_\nu = -\frac{1}{3}k^2\delta_\nu - \frac{4}{3}k^2\phi + 4\ddot{\psi} - \frac{4}{3}k^2\sigma_\nu. \tag{3.46}$$

The first term on the right hand side describes relativistic pressure, the second one is the gravitational force, third one represents the fact that when ψ is locally changed, then the neutrino wavelength will change. This process is similar to integrated Sachs-Wolfe effect. This will locally change the blackbody radiation temperature and density. And the last term describes the shear of the neutrinos. The shear is not considered on the super-horizon scales, where neutrinos are static and perturbations are proportional to the metric perturbations. Shear becomes significant on scales smaller than horizon, were it acts as the viscosity in the fluid, that damps the energy density and velocity perturbations. More generally, the energy of smaller multipoles will decrease, giving rise to the energy of higher multipoles. This can be explained in a way that locally there would be many flows randomly coming from different direction, but the density contrast on average would be zero. The equation for density contrast is similar to the equation for photon evolution. The only difference is that before recombination photons do not experience shear. We have also considered here baryon to photon ratio to be small, so we can ignore photon collisions with baryons.

3.6 Massive neutrinos

Massive neutrinos are also collisionless. The unperturbed density and pressure for massive neutrinos are

$$\bar{\rho}_\nu = a^{-4}\int q^2 dq d\Omega \varepsilon f_0(q) = 4\pi a^{-4}\int q^2 dq \varepsilon f_0(q) \tag{3.47}$$

$$\bar{P}_\nu = \frac{1}{3}a^{-4}\int q^2 dq d\Omega \frac{q^2}{\varepsilon} f_0(q) = \frac{4\pi}{3}a^{-4}\int q^2 dq \frac{q^2}{\varepsilon} q f_0(q) \tag{3.48}$$

where $\varepsilon = \varepsilon(q,\tau) = \sqrt{q^2 + m_\nu^2 a^2}$. For perturbations we will have

$$\delta\rho = a^{-4}\int q^2 dq d\Omega \varepsilon f_0(q)\Psi \tag{3.49}$$

$$\delta P = \frac{1}{3}a^{-4}\int q^2 dq d\Omega \frac{q^2}{\varepsilon} f_0(q)\Psi \tag{3.50}$$

$$\delta T_i^0 = a^{-4}\int q^2 dq d\Omega q n_i f_0(q)\Psi \tag{3.51}$$

$$\Sigma_j^i = a^{-4}\int q^2 dq d\Omega \frac{q^2}{\varepsilon}\left(n_i n_j - \frac{1}{3}\delta_{ij}\right) f_0(q)\Psi \tag{3.52}$$

For massive neutrinos ε and q are not equal anymore, which is why we can not integrate out the q-dependence of $f(q,\tau)$ from the distribution function. Instead, we can use the Legendre expansion of the perturbation Ψ:

$$\Psi\left(\vec{k},\hat{n},q,\tau\right) = \sum_{l=0}^{\infty}\left(-i^l\right)(2l+1)\Psi_l(\vec{k},q,\tau)P_l(\hat{k}\cdot\hat{n})\ , \tag{3.53}$$

The perturbed energy density, pressure, velocity gradient and anisotropic stress can be written as

$$\delta\rho = 4\pi a^{-4}\int q^2 dq \varepsilon f_0(q)\Psi_0 \tag{3.54}$$

$$\delta P = \frac{4\pi}{3}a^{-4}\int q^2 dq \frac{q^2}{\varepsilon} f_0(q)\Psi_0 \tag{3.55}$$

$$(\bar{\rho}+\bar{P})\theta = 4\pi k a^{-4}\int q^2 dq q f_0(q)\Psi_1 \tag{3.56}$$

$$(\bar{\rho}+\bar{P})\sigma = \frac{8\pi}{3}a^{-4}\int q^2 dq \frac{q^2}{\varepsilon} f_0(q)\Psi_2\ . \tag{3.57}$$

The Vlasov equation (3.30)

$$\dot{\Psi}_0 = -\frac{qk}{\varepsilon}\Psi_1 - \dot{\phi}\frac{d\ln f_0}{d\ln q} \tag{3.58}$$

$$\dot{\Psi}_1 = \frac{qk}{3\varepsilon}(\Psi_0 - 2\Psi_2) - \frac{\varepsilon k}{3q}\psi d\ln f_0 d\ln q, \tag{3.59}$$

$$\dot{\Psi}_l = \frac{qk}{(2l+1)\varepsilon}\left[l\Psi_{(l-1)} - (l+1)\Psi_{(l+1)}\right], l \geq 2\ . \tag{3.60}$$

When neutrinos are well inside the non-relativistic regime, which is true when the distribution function $f_0(q)$ is non-negligible for neutrinos with momentum $q \ll \varepsilon \sim am$, (3.54)-(3.57) equations show that δP_h and $(\bar{\rho}_h + \bar{P}_h)\sigma_h$ are much bigger than $\delta\rho_h$. In this case the continuity and Euler equations

$$\dot{\delta}_\nu = -\theta_\nu + 3\dot{\phi}, \tag{3.61}$$

$$\dot{\theta}_\nu = -\frac{\dot{a}}{a}\theta_\nu + k^2\psi, \tag{3.62}$$

can be combined to give

$$\ddot{\delta}_\nu + \frac{\dot{a}}{a}\delta_\nu = -k^2\psi + 3(\ddot{\phi} + \frac{\dot{a}}{a}\dot{\phi}) \ . \tag{3.63}$$

Neutrinos in the sub-eV mass range become non-relativistic in the matter dominated universe, where ϕ and ψ are approximately constants. Then, the solution to the last equation is

$$\delta_\nu = A\ln\tau + B - \frac{(k\tau)^2}{6}\psi \tag{3.64}$$

where A and B are integration constants. For $k > k_{nr}$, which means the modes that are inside the horizon at the time of the non-relativistic transition, the last term in the equation dominates and the density contrast for neutrinos will be smaller than δ_{cdm}. But after long time the third and first term will become equal to each other, and massive neutrinos will start to behave as CDM on all scales. That time is not reached today yet. For $k < k_{nr}$, the modes are outside the horizon at the time of non-relativistic transition and the density contrast of neutrinos is time-independent. After the horizon crossing, it becomes equal to the density contrast of CDM in a very short time. So, the density contrast of neutrinos equals to that of CDM on scales $k < k_{nr}$, and is smaller on scales $k > k_{nr}$.

3.7 The growth of density fluctuations

Massive neutrinos affect the growth of perturbations in two ways. During the matter dominated era, on scales smaller than the free streaming scale, neutrinos do not contribute to clustering. But they still contribute to the background expansion of the Universe through the Friedmann equation. This means that on these scales the growth function will grow slower than a. It is possible to find how δ_{cdm} depends on scale a. For that let's at first write down the equations for neutrinoless universe. For the cold dark matter density contrast from the continuity and Euler equations, we can write

$$\ddot{\delta}_{cdm} + \frac{\dot{a}}{a}\dot{\delta}_{cdm} = -k^2\psi + 3\left(\ddot{\phi} + \frac{\dot{a}}{a}\dot{\phi}\right). \tag{3.65}$$

Well inside the Hubble radius, the first term in (3.65) will dominate. If the shear can be neglected, then $\phi = \psi$. Using the Poisson equation, (3.65) will be

$$\ddot{\delta}_{cdm} + \frac{\dot{a}}{a}\dot{\delta}_{cdm} = 4\pi G a^2 \delta\rho \tag{3.66}$$

where $\delta\rho$ is the total density perturbation. For cold dark matter, using $\delta\rho \propto \delta_{cdm} a^{-1}$ and $a \propto \tau^2$, the equation will become

$$\ddot{\delta}_{cdm} + \frac{2}{\tau}\dot{\delta}_{cdm} - \frac{6}{\tau^2}\delta_{cdm} = 0 \tag{3.67}$$

This has two solutions $\delta_{cdm} \propto \tau^2$ and τ^{-3}. If we neglect the decaying mode, we will get $\delta_{cdm} \propto a$. If we have massive neutrinos, then well inside the matter-domination era on scales smaller then non-relativistic scale, these neutrinos will not contribute to the Poisson equation, thus we have $\delta\rho_\nu = 0$ and $\delta\rho = (\bar{\rho}_{cdm} + \bar{\rho}_b)\delta_{cdm}$. But they will contribute to the expansion of the Universe through (3.4). We can introduce a new quantity, which is the ratio of neutrinos to the total matter density,

$$f_\nu \equiv \frac{\rho_\nu}{(\rho_{cdm} + \rho_b + \rho_\nu)} = \frac{\Omega_\nu}{\Omega_m} \, . \tag{3.68}$$

With the presence of neutrinos, Eq. (3.67) becomes different:

$$\ddot{\delta}_{cdm} + \frac{2}{\tau}\dot{\delta}_{cdm} - \frac{6}{\tau^2}(1 - f_\nu)\,\delta_{cdm} = 0 \, . \tag{3.69}$$

From this equation, we get for the CDM density contrast

$$\delta_{cdm} \propto a^{1-(3/5)f_\nu} \, . \tag{3.70}$$

Also, from the Poisson equation we find

$$k^2\phi \propto a^{-(3/5)f_\nu} \, , \tag{3.71}$$

which, as expected, gives $\phi = const$ for $f_\nu = 0$. For $f_\nu \neq 0$, structure growth and the gravitational potential are suppressed, because one of the matter components (massive neutrinos) contributes to the homogeneous expansion of the Universe, but not to the clustering.

Chapter 4

Effects of Neutrino Mass on Observables

4.1 Adding a new component to the universe

Neutrinos become non-relativistic at redshift $z_{nr} \approx 200 m_\nu/(0.1eV)$, after the decoupling of CMB photons, which happened at $z_{\gamma d} \approx 1090$. Therefore, their small mass does not directly affect the perturbation dynamics at that the time of last scattering. However, their effect can still be observed in the CMB lensing, which is caused by the structure formation.

After the non-relativistic transition, neutrinos effectively contribute as a matter component with some Ω_ν. If were to simply add this to the right hand side of the Friedman equation describing a flat universe today,

$$\Omega_M + \Omega_\Lambda = 1 \ , \tag{4.1}$$

then the sum would be greater than one. As already discussed, the observations show that the Universe is spatially flat, and the right hand side in the equation above must remain the same. Thus we can only change the relative densities, and this can be done in more than one way, depending on how one wants to compare observables calculated with and without massive neutrinos. Note that in all cases we have the usual three flavours of neutrinos, but their masses can vary. In particular, let us discuss two examples:

- **Case (a):** Here one assumes that the universe started at some early time with a fixed density of CDM, baryons, cosmological constant, relativistic neutrinos and photons. If neutrinos are massive, at some point they will start contributing to the matter density. In terms of the parameters that we observe today, it means keeping $\omega_b = \Omega_b h^2$,

$\omega_{cdm} = \Omega_{cdm}h^2$, $\omega_\Lambda = \Omega_\Lambda h^2$ fixed, and adding $\Omega_\nu h^2$ to the total density today. Then, for a flat universe, we must have

$$\frac{\omega_b + \omega_{cdm} + \omega_\Lambda + \Omega_\nu h^2}{h^2} = 1 \ , \tag{4.2}$$

which we can use to solve for h. In other words, here one fixes the physical densities of *CDM*, b and Λ, but adjusts h depending on the neutrino mass. This seems like a reasonable approach, but it assumes that we somehow know the initial densities, but don't now the current expansion rate. In practice, the situation is often the opposite – we infer the initial densities, based on the observations that include current expansion rate.

- **Case (b):** Here one keeps h, Ω_Λ, and Ω_b fixed, which means that the total matter fraction $\Omega_M = \Omega_{cdm} + \Omega_b + \Omega_\nu$ is also fixed. This means that when Ω_ν is increased, Ω_{cdm} is decreased. We effectively fix the total dark matter fraction today, and any contribution from massive neutrinos will be at the cost of having less CDM.

We will adopt Case (b) for the main calculations in this thesis, because it is consistent with the assumptions made in deriving the principal components of the modified gravity functions μ and γ that will be introduced later.

4.2 The matter power spectrum

The effect of the neutrino mass on the matter power spectrum, $P(k) = 4\pi\delta_M^2(k)$, is demonstrated in Fig. 4.1. The figure compares $P(k)$ of the ΛCDM model with three other modes in which neutrinos have masses of 0.05, 0.1 and 0.5 eV. These spectra were calculated numerically, using the publicly available code CAMB [19]. As one can see in this figure, the power spectrum on small scales is suppressed when we increase the neutrino mass. On large scales, however, the different curves practically coincide. Let us understand the shapes of the curves in Fig. 4.1 analytically by comparing spectra in two models of the universe: one with massless neutrinos and one with massive neutrinos.

Let us at first consider large scales ($k < k_{nr}$). On these scales both neutrinos and CDM perturbations are outside the horizon when neutrinos are still relativistic and neither density contrast is growing. When they enter the horizon during the matter era, the neutrinos are

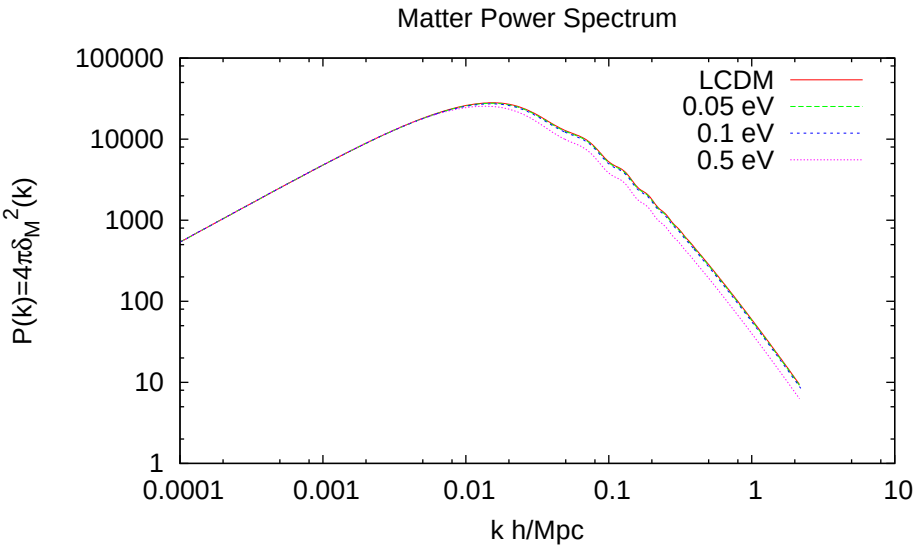

Figure 4.1: The matter power spectrum for different neutrino masses, case b.

non-relativistic and contribute as a matter component to the growth of structures through the Poisson equation. They also contribute as a matter component to the expansion of the universe. As a result, the density contrast δ_{cdm} grows proportionally to the scale factor a. The effect is the same as if neutrinos were massless – they affect neither the growth nor the expansion. Therefore, on these scales, the two matter power spectra will be identical.

On smaller scales, for modes that enter the horizon before z_{nr}, i.e. $k > k_{nr}$, the matter power spectra are different. Let us at first discuss the case after matter-radiation equality, but before the non-relativistic transition of neutrinos, i.e. $a_{eq} < a < a_{nr}$. The density contrast of cold dark matter starts growing at a_{eq}, but equality happens at different times for the two models. We have

$$\frac{a_{eq}}{a_0} = \frac{\Omega_r}{\Omega_b + \Omega_{cdm}} = (1 - f_\nu)^{-1} \frac{\Omega_r}{\Omega_m} \,, \tag{4.3}$$

where Ω_r includes photons and 3 massless neutrinos. As both models have the same values for Ω_r and Ω_m, the equality takes place at different times:

$$a_{eq}^{f_\nu} / a_{eq}^{f_\nu = 0} = (1 - f_\nu)^{-1} \,. \tag{4.4}$$

This equation is written for the time of matter-radiation equality, but it is true at any a in the range $a_{eq} < a < a_{nr}$. This means that before the non-relativistic transition, $a \leqslant a_{nr}$, the two models have the same dependence of δ_{cdm} on the scale factor a, but a/a_{eq} is different. Thus, the density contrast will be given by

$$\delta_{cdm}^{f_\nu}[a] = \delta_{cdm}^{f_\nu=0}[(1-f_\nu)a] \tag{4.5}$$

After the non-relativistic transition, $a > a_{nr}$, and on scales smaller than free-streaming, $k > k_{FS}$, the relation of the two density contrasts will be further modified. If we write down their dependence on the scale factor, given by (3.70), then for $\delta_{cdm}^{f_\nu}$ today we will get

$$\delta_{cdm}^{f_\nu}[a_0] = \left(\frac{a_0}{a_{nr}}\right)^{1-(3/5)f_\nu} \delta_{cdm}^{f_\nu}[a_{nr}], \tag{4.6}$$

where a_{nr} describes the time, at which the massive neutrinos became non-relativistic. We can relate density contrasts of two models to each other, using the relations Eq. (4.5) and Eq. (4.6). We will get

$$\delta_{cdm}^{f_\nu}[a_0] = \left(\frac{a_0}{a_{nr}}\right)^{1-(3/5)f_\nu} \delta_{cdm}^{f_\nu=0}[(1-f_\nu)a_{nr}] \ , \tag{4.7}$$

where a_0 is the scale factor today. If we suppose that in the model with massless neutrinos $\delta_{cdm} \propto a$, then for two different scale factors we can write

$$\frac{\delta_{cdm}^{f_\nu=0}[a_0]}{a_0} = \frac{\delta_{cdm}^{f_\nu=0}[(1-f_\nu)a_{nr}]}{(1-f_\nu)a_{nr}} \ . \tag{4.8}$$

Eq. (4.7) will be

$$\delta_{cdm}^{f_\nu}[a_0] = \left(\frac{a_0}{a_{nr}}\right)^{-(3/5)f_\nu} (1-f_\nu)\delta_{cdm}^{f_\nu=0}[a_0] \ . \tag{4.9}$$

In reality, δ_{cdm} is not proportional to a, and instead we can use the semi-analytical result [6]

$$\delta_{cdm}^{f_\nu=0}[a_0] \simeq \left(\frac{a_0}{(1-f_\nu)^{1/2}a_{nr}}\right) \delta_{cdm}^{f_\nu=0}[(1-f_\nu)a_{nr}] \ . \tag{4.10}$$

Using this we can get the ratio of density contrasts of massive and massless neutrino models today:

$$\frac{\delta_{cdm}^{f_\nu}[a_0]}{\delta_{cdm}^{f_\nu=0}[a_0]} = (1-f_\nu)^{1/2}\left(\frac{a_0}{a_{nr}}\right)^{-(3/5)f_\nu} . \tag{4.11}$$

Using the equation

$$P(k) = \begin{cases} \langle \delta^2_{cdm} \rangle & k < k_{nr} \\ [1 - \Omega_\nu/\Omega_M]^2 \langle \delta^2_{cdm} \rangle & k < k_{FS} < k_{nr} \end{cases}$$

for the matter power spectrum, we can get their ratio, too

$$\frac{P(k)^{f_\nu}}{P(k)^{f_\nu=0}} = (1 - f_\nu)^3 \left(\frac{a_0}{a_{nr}} \right)^{-(6/5)f_\nu} . \tag{4.12}$$

Let us now consider the case, when $k_{nr} < k < k_{FS}$, i.e. scales smaller than the non-relativistic transition scale, but larger than the free-streaming length. In this case Eq. (4.5) is correct again for $a \leqslant a_{nr}$. The relation of density contrasts at different times will be given by

$$\delta^{f_\nu}_{cdm}[a_0] = \left(\frac{a_0}{a_{nr}} \right) \delta^{f_\nu}_{cdm}[a_{nr}] . \tag{4.13}$$

From this and Eq. (4.8) it follows that

$$\delta^{f_\nu}_{cdm}[a_{nr}] = \delta^{f_\nu=0}_{cdm}[(1 - f_\nu)a_{nr}] = \frac{(1 - f_\nu)a_{nr}}{a_0} \delta^{f_\nu}_{cdm}[a_0] . \tag{4.14}$$

If we again use the semi-analytical result for the density contrast ratio, we will have

$$\delta^{f_\nu}_{cdm}[a_0] = (1 - f_\nu)\delta^{f_\nu=0}_{cdm}[a_0] , \tag{4.15}$$

$$\frac{\delta^{f_\nu}_{cdm}[a_0]}{\delta^{f_\nu=0}_{cdm}[a_0]} = (1 - f_\nu)^{1/2} \left(\frac{a_0}{a_{nr}} \right)^{-(3/5)f_\nu} . \tag{4.16}$$

This means that the ratio of matter power spectra in this case is

$$\frac{P(k)^{f_\nu}}{P(k)^{f_\nu=0}} = (1 - f_\nu) . \tag{4.17}$$

Both the numerical and the analytical results in this section show that the matter power spectrum is reduced in the case of massless neutrinos. When the matter-radiation equality is postponed, modes crossing the horizon in the matter-dominated era have lesser time for density perturbations to grow. Therefore, the amplitude of the perturbations on this small scales will be small. In addition, perturbations are suppressed on scales smaller than the free-streaming length.

4.3 Cosmic microwave background anisotropies

CMB temperature fluctuations were first measured by COBE satellite in 1992 [20], and significantly improved by subsequent experiments, most importantly by WMAP [18]. Given a measurement of the CMB temperature anisotropy in various directions on the sky, one can define the two point correlation function as

$$C(\theta) = \langle \Delta(\hat{n}_1)\Delta(\hat{n}_2) \rangle \ . \tag{4.18}$$

It can be further expanded it into Legendre functions

$$C(\theta) = \frac{1}{4\pi} \sum_{l=0}^{\infty} (2l+1) C_l P_l(\hat{n}_1 \cdot \hat{n}_2) \ , \tag{4.19}$$

with coefficients C_l being the so-called *angular power spectrum*. In Fig. 4.2, we show the CMB spectra as predicted by the ΛCDM model with massless neutrinos, as well as models with neutrino masses of 0.05, 0.1 and 0.5 eV. The curves in the figure are calculated numerically using CAMB [19].

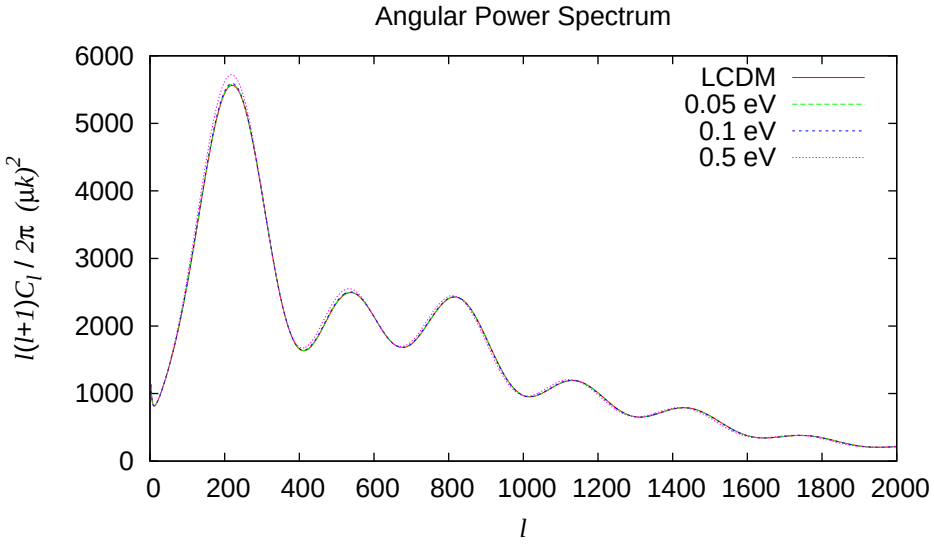

Figure 4.2: Angular power spectrum for different neutrino masses, case b.

One can try to understand the differences between different lines in Fig. 4.2 as follows. For the neutrino masses that we have considered, the neutrinos are still relativistic at the time of radiation-matter equality. This means that the equality occurs later than in the universe with massless neutrinos, which affects the CMB anisotropy spectrum in two ways. First, the first acoustic peak is enhanced, because of the so-called early integrated Sachs-Wolfe (EISW) effect. Gravitational potentials evolve during radiation domination, changing the energy of photons traveling through them. Increasing the amount of radiation in the universe results in an increase in the EISW contribution to the CMB temperature fluctuations due to increased rate of gravitational potential decay [21]. Thus, the fluctuations near the first acoustic peak will increase. Secondly, increasing the mass of neutrinos reduces the distance to the last scattering surface, which is inversely proportional to the peak position. Hence, the position of the first peak will move towards the bigger ls [21]. As we can see in the figure, the first effect is more visible for the small neutrino masses that we are interested in.

Chapter 5

Principal Components of Modified Linear Growth

Following Zhao et al [1] we focus on perturbations in the Newtonian gauge with metric potentials ψ and ϕ, defined in Eq. (3.7) and assume that the matter perturbations obey the standard conservation equations. Namely, we have

$$\delta' + \frac{k}{aH}\theta - 3\phi' = 0 \tag{5.1}$$

$$\theta' + \theta - \frac{k}{aH}\psi = 0\,, \tag{5.2}$$

where the prime denotes differentiation with respect to $\ln a$, and $H \equiv a^{-1}da/dt$, with t being the physical time and where we have specialized to cold dark matter (for the sake of simplicity we ignore radiation or baryonic effects, which can be included if relevant).

One needs two additional equations to close the system for the four variables ϕ, ψ, δ and θ. These are normally provided by a theory of gravity, which prescribes how the two metric potentials relate to each other, and how they are sourced by the matter perturbations. In Zhao et al [1], it was proposed to consider a general way of allowing for alternatives to GR, and the system of equations was closed by introducing two general functions of scale and time defined as:

$$\gamma(k,a) \equiv \frac{\phi}{\psi} \tag{5.3}$$

$$\mu(k,a) \equiv -\frac{1}{4\pi G a^2}\frac{k^2\psi}{\rho\Delta}\,, \tag{5.4}$$

where $\Delta \equiv \delta + 3aH\theta/k$ is the comoving matter density perturbation. Eqs. (5.1)-(5.4) form a closed system, that can be used to calculate the evolution of perturbations for any given functions μ and γ, and were extensively discussed in [22].

Let us comment on some of the properties of functions μ and γ. By design, in GR, and in a universe made of dust (CDM) and a cosmological constant (Λ), $\mu = \gamma = 1$. Departure of μ and/or γ from unity can happen if, for example, DE is dynamical (because of the clustering of DE) or if it has a non-negligible anisotropic stress. Alternatively, as will be discussed later in the thesis, one could have $\mu \neq 1$ due to a significant fraction of massive neutrinos, which free stream on small scales. Finally, alternative gravity models generally predict scale- and time-dependent μ and/or γ [23].

The main benefit of introducing μ and γ, is that it allows for model-independent tests of departures of linear growth of perturbations from that in adiabatic GR+ΛCDM. Any measured deviation of either μ or γ from unity would signal that an ingredient in the ΛCDM model needs to be modified. Additionally, since any departure of growth from ΛCDM on linear scales corresponds to some form of μ and γ, these two functions can be used as a way of storing information from observations in a model-independent way. It is this latter use of the parameterization that is explored in this thesis.

5.1 Principal component analysis of μ and γ

In [1], Zhao et al have investigated how well the functions $\mu(a,k)$ and $\gamma(a,k)$ can be constrained by future surveys, in particular CMB measurements from Planck and weak lensing shear and galaxy surveys from LSST. They treat μ and γ as unknown functions of both time and wavenumber, and bin them on a grid in the (z,k) space (notice that we are using the redshift z as the time variable). With m z-bins and n k-bins, the values of the functions μ and γ at the grid points can be treated as $2 \times m \times n$ parameters, μ_i and γ_i. In addition, they also vary the usual cosmological parameters: $\Omega_b h^2$, $\Omega_{cdm} h^2$, Hubble constant h, optical depth τ, spectral index n_S and amplitude A_S, as well as the DE equation state, binned over the same m grid points in z as μ and γ, and N_b bias parameters. They then use the Fisher matrix formalism to estimate the covariance of the $2 \times m \times n$ parameters after marginalizing over the usual cosmological parameters.

Here we explain what was done in Zhao et al. Suppose one wants to know how well

a given combination of experiments will measure μ, with other parameters marginalized over. The relevant quantity is the μ block of the covariance matrix:

$$C_{ij} \equiv \langle (\mu_i - \bar{\mu}_i)(\mu_j - \bar{\mu}_j) \rangle \ , \tag{5.5}$$

where $\bar{\mu}_i$ is the fiducial value, which is in the case of a forecast plays the role of the best fit value. Since the individual pixels of μ are highly correlated, the covariance matrix (5.5) will be non-diagonal, and the value of μ in any particular bin would be practically unconstrained. The PCA is a way to decorrelate the parameters and find their linear combinations that are best constrained by data. Namely, we solve an eigenvalue problem to find a matrix W that diagonalizes C:

$$C = W^T \Lambda W \ ; \ \ \Lambda_{ij} = \lambda_i \delta_{ij} \ , \tag{5.6}$$

where λ_i's are the eigenvalues. Smaller values of λ_i correspond to the better constrained linear combinations of μ's:

$$\alpha_i = \sum_{j=1}^{m \times n} W_{ij} (\mu_j - \bar{\mu}_j) \ . \tag{5.7}$$

One can think of α's as the new set of uncorrelated parameters obtained by a rotation of μ's, with the error on α_i given by $\sqrt{\lambda_i}$. In practice, one finds that only a few of the α's are well constrained (i. e. their λ's are small), while most are essentially unconstrained. This is the main benefit of performing a PCA – it takes a function with many (infinite) degrees of freedom and isolates their few linear combinations that can be constrained by a given experiment. By construction, $W^T W = I$, so Eq. (5.7) can be inverted as

$$\mu_i - \bar{\mu}_i = \sum_{j=1}^{m \times n} W_{ij} \alpha_j \ . \tag{5.8}$$

In the above, i labels a point on the (z,k) grid. Thus, taking the continuous limit and using $\mu = 1$ as the fiducial value, we can formally rewrite this as

$$\mu(z,k) = 1 + \sum_j \alpha_j W_j(z,k) \ , \tag{5.9}$$

which is an expansion of μ into an orthogonal basis of eigenvectors $W_j(z,k)$. The best constrained eigenvectors $W_j(z,k)$ can be plotted as surfaces in (k,z) space, with their shapes indicating the kind of patterns that experiments are most likely to constrain.

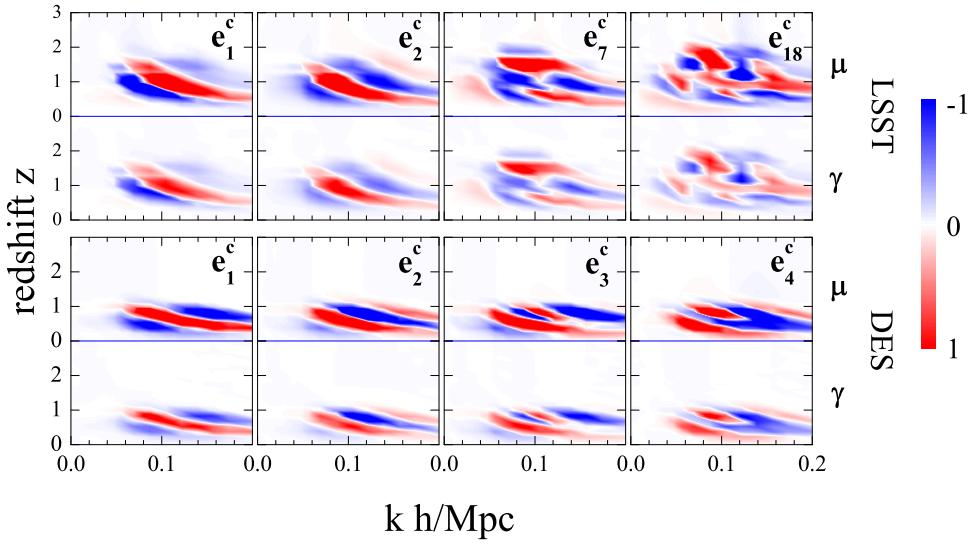

Figure 5.1: The combined eigenmodes of μ and γ as pairs of (k,z) surfaces for data sets including LSST or DES data.

If one is interested in seeing how sensitive data is to *any* departure from "normal" growth, then rather than trying to constrain μ or γ individually, one wants to know if either function is deviating from unity, without specifying which. To address this question, Zhao et al considered the combined principal components of μ and γ. Namely, they follow the same procedure as described above, except now they diagonalize the block of the Fisher matrix containing μ *and* γ pixels. The eigenmodes in this case are no longer single surfaces in (k,z) space, instead each mode can be represented as two surfaces, one for each of μ and γ. Some representative eigenmodes, represented as pairs of surfaces in the (k,z) space, are shown in Fig. 5.1. We note that Zhao et al used the flatness prior, $\Omega = 1$, and also limited the range of each μ-pixel to $0 < \mu < 2$.

5.2 Modified growth from massive neutrinos

As we discussed in Chapter 3, neutrino mass alters the growth of cosmological perturbations, as compared to that in ΛCDM. Neutrino mass does not produce any additional anisotropic stress. Hence, in terms of the MG functions, $\gamma = 1$ for massive neutrinos. On

the other hand, μ has a non-trivial form. To see this, let us look at the Poisson equations with massive neutrinos:

$$k^2\phi = -4\pi G a^2 \sum_i \rho_i \Delta_i = -4\pi G a^2 (\rho_{cdm}\Delta_{cdm} + \rho_B \Delta_B + \rho_\nu \Delta_\nu) \ . \tag{5.10}$$

We can compare this to the one in ΛCDM:

$$k^2\phi = -4\pi G a^2 (\rho_{cdm}\Delta_{cdm} + \rho_B \Delta_B) \ . \tag{5.11}$$

On the other hand, from the definition of μ, we have

$$k^2\phi = -4\pi G a^2 \mu \rho_M \Delta_{cdm} \tag{5.12}$$

where ρ_M is the total matter density, including ρ_{cdm} and ρ_B. In other words, this parametrization is based on the fact that in ΛCDM $\Delta_B = \Delta_{cdm}$ at redshifts probed by the surveys we consider. From this definition, we can read off the form of μ for the case with massive neutrinos:

$$\mu_\nu(k,z) = \frac{\rho_{cdm}\Delta_{cdm} + \rho_B \Delta_B + \rho_\nu \Delta_\nu}{\rho_M \Delta_{cdm}} \tag{5.13}$$

where $z = 1/a - 1$ is the redshift, and $\rho_M = \rho_{cdm} + \rho_B + \rho_\nu$. Note that by design μ_ν approaches unity on large scales, where neutrino free-streaming is negligible, and departs from unity below the free-streaming scale. We evaluate Eq. (5.13) numerically using CAMB, and contours of constant μ_ν in (k,z)-plane are shown in Fig. 5.2.

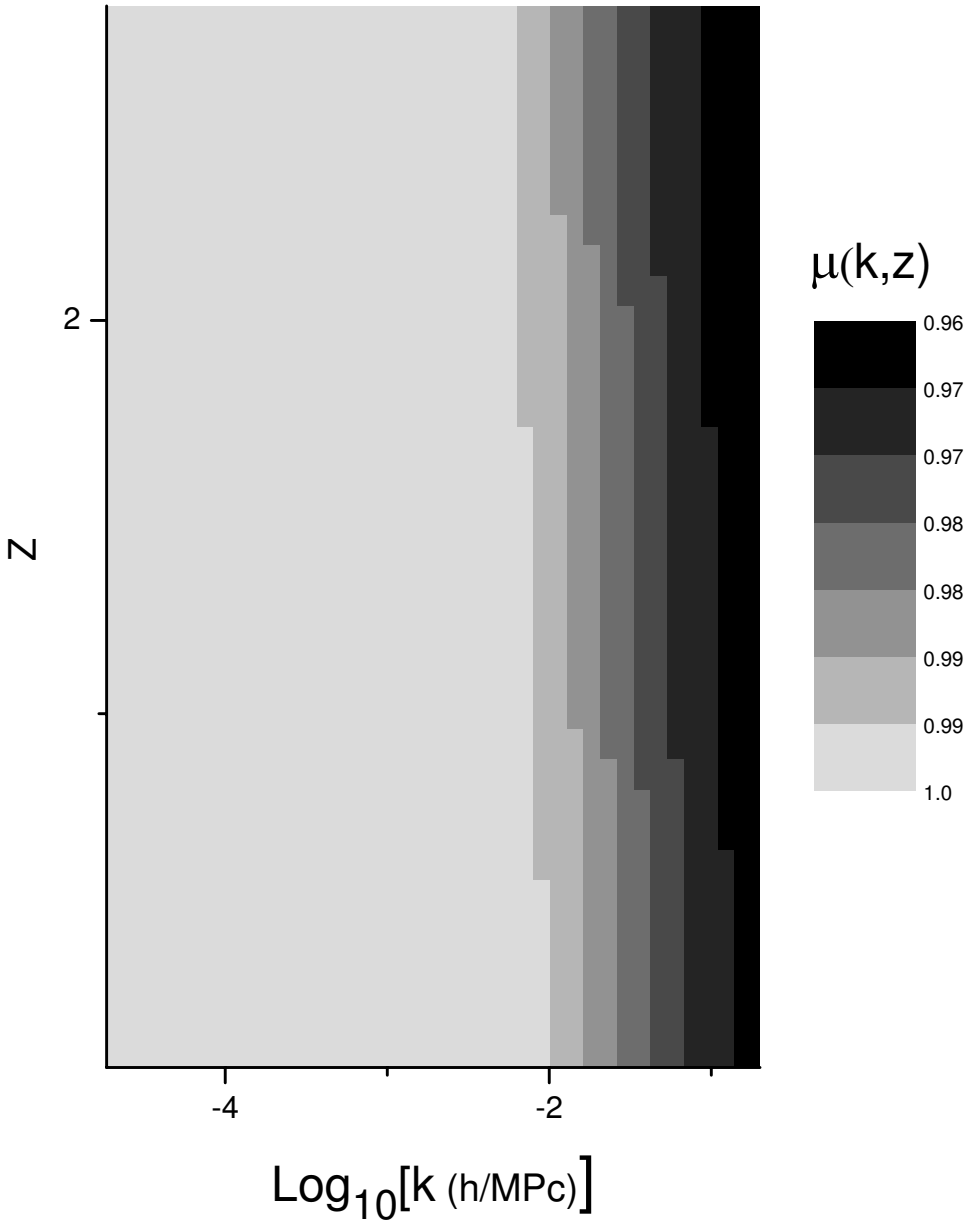

Figure 5.2: Contours of $\mu_\nu(k,z)$ for massive neutrinos as defined in Eq. (5.13). Note that for small $k < k_{FS}$ the function approaches unity. Also note that the free-streaming scale k_{FS} depends on z.

Chapter 6

Uncertainty in m_ν from PCA of Modified Growth

6.1 From eigenmodes of MG to uncertainties on neutrino mass

As mentioned in the previous Chapter, parameterizing departures from the ΛCDM growth in terms of μ and γ can be a convenient way of storing information in a model-independent way. Here we will illustrate how, for example, the information stored in these functions can be retrieved to calculate forecasted uncertainties on the sum of the three neutrino masses. We will use the formalism of Section 1.6.

Let μ_i denote collectively the values of μ and γ on a grid in (k,z). These could be the $2\times n\times m$ pixels considered in Zhao et al. Now suppose we could measure μ_i from a set of observations. Then, formally, we could think of μ_i's as a new set of observables, which contain all the information that you could extract about the growth of perturbations on linear scales. Given this assumption, we can calculate the Fisher matrix in any set of parameters p_a that affect the linear growth as

$$F_{ab} = \sum_{ij} \frac{\partial \mu_i}{\partial p_a} \frac{1}{C_{ij}} \frac{\partial \mu_j}{\partial P_b} \ , \tag{6.1}$$

where C_{ij} is the covariance of the MG pixels. We can now diagonalize C_{ij} and rewrite the

above Fisher matrix as

$$F_{ab} = \sum_k \alpha_k^{(a)} \alpha_k^{(b)} \lambda_k^{-1} \ , \tag{6.2}$$

where λ_k are the eigenvalues of C_{ij}, and coefficients $\alpha_k^{(a)}$ are obtained by decomposing derivatives of μ_i into the basis of orthogonal eigenmodes shown in Fig. 5.1:

$$\frac{\partial \mu_j}{\partial p_a} = \sum_i \alpha_i^{(a)} W_{ij} \ , \tag{6.3}$$

where

$$\alpha_k^{(a)} = \sum_i \frac{\partial \mu_i}{\partial p_a} W_{ik}^T \ . \tag{6.4}$$

Given a set of eigenmodes and eigenvalues provided by Zhao et al, Eq. (6.2) can be used to find uncertainties any set parameters if it is possible to evaluate the partial derivatives in Eq. (6.3).

Specifically, this method can be applied to derive the uncertainty in the measurement of the sum of neutrino masses m_ν. Namely, we have

$$\sigma_{m_\nu}^{-2} = F_{m_\nu m_\nu} = \sum_k \alpha_k^{(m_\nu)} \alpha_k^{(m_\nu)} \lambda_k^{-1} \ , \tag{6.5}$$

where

$$\alpha_k^{(m_\nu)} = \sum_i \frac{\partial \mu_i}{\partial m_\nu} W_{ik}^T \ . \tag{6.6}$$

The derivative of μ_ν with respect to m_ν can be evaluated numerically using CAMB [19]. When $m_\nu \neq 0$, $\gamma = 1$ and μ is given by (5.13). Namely, we calculate

$$\frac{\partial \mu_\nu(k,z)}{\partial m_\nu} \to \frac{\mu_\nu(m_\nu + \Delta m_\nu) - \mu_\nu(m_\nu)}{\Delta m_\nu} \tag{6.7}$$

for a Δm_ν, that is sufficiently small for the result to converge. To be consistent with the fiducial model used in Zhao et al, we choose the ΛCDM fiducial value $m_\nu = 0$, and we checked that the derivative converges for $\Delta m_\nu = 0.05$eV.

The advantage of working with eigenmodes, as opposed to the complete set of pixels, is that most of the eigenmodes are poorly constrained. That is, most of them have very large eigenvalues λ_k and their contribution to the sum in Eq. (6.2) is negligible. Hence, it may be possible to only work with a small subset of eigenmodes. We will check this in the next section.

6.2 Results

We calculated the expected uncertainty in the measurement of the neutrino mass from the eignemodes of MG using Eq. (6.2) of the previous section. The forecasted error is $\sigma_\nu = 0.07$eV, which is very close to the error forecast of 0.05eV for the combination of Planck and LSST obtained in [25] by directly calculating all the observables. Note that the difference between our result and theirs is well within typical uncertainties involved in Fisher forecasts.

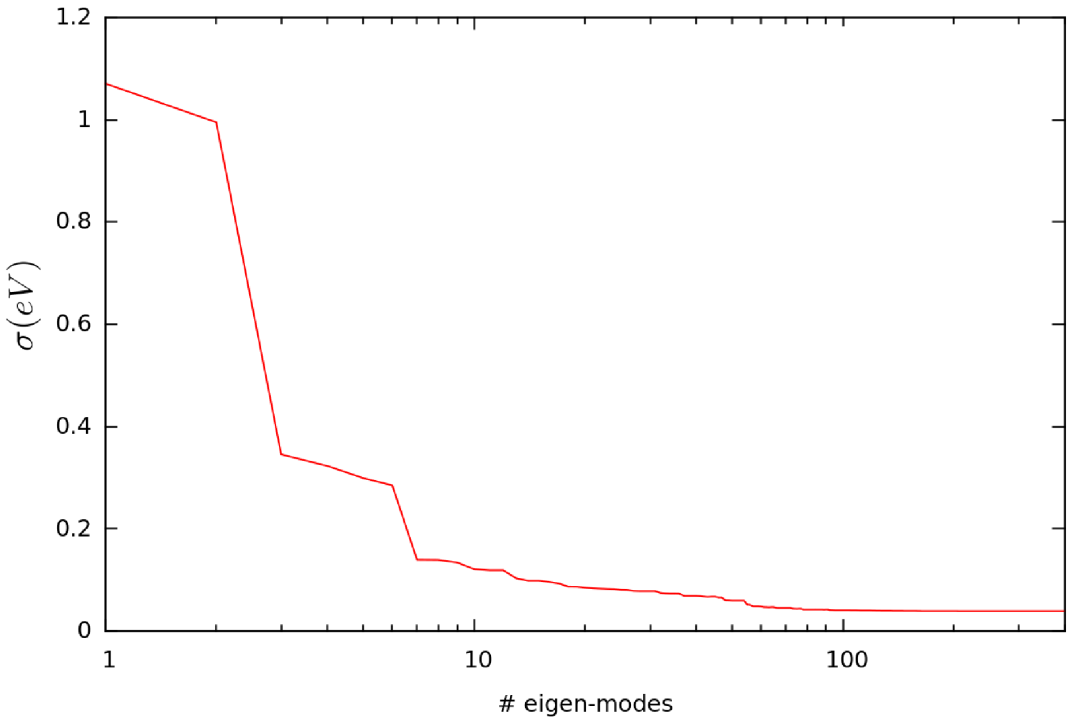

Figure 6.1: The forecasted uncertainty in the measurement of the sum of masses of the three neutrinos derived from eignemodes of MG, as a function of the number of included modes.

In Fig. 6.1 we demonstrate how strongly our forecasted error depends on the number of eignemodes included in the analysis. We can see that at least 10 eigenmodes are needed to get within 100% of the "correct" error, and about 40 to get within 10%. Clearly, this is much less than the total number of the eigenmodes (which was equal to 800 for the set we

used), and also much less than the total number of observables available from LSST and Planck (which is of the order of many thousands of independent data points).

Chapter 7

Summary

In this thesis, we studied the effects of neutrino mass on cosmological observables. We also demonstrated how information stored in the principle components of modified gravity can be used to calculate the accuracy with which neutrino mass can be measured. While more investigation is needed to make definitive forecasts of neutrino mass constraints from PCA of MG, this work shows that using the existing eignemodes from Zhao et al [1] effectively reproduces the constraints obtained by direct methods in [25]. We expect such methods will be of use to the cosmological community, as they significantly simplify the process of error forecasts for various models of modified gravity.

Bibliography

[1] G. B. Zhao, L. Pogosian, A. Silvestri and J. Zylberberg, Phys. Rev. Lett. **103**, 241301 (2009) [arXiv:0905.1326 [astro-ph.CO]].

[2] B. T. Cleveland *et al.*, Astrophys. J. **496**, 505 (1998).

[3] [ALEPH Collaboration and DELPHI Collaboration and L3 Collaboration and], Phys. Rept. **427**, 257 (2006) [arXiv:hep-ex/0509008].

[4] Y. Fukuda *et al.* [Super-Kamiokande Collaboration], Phys. Rev. Lett. **81**, 1562 (1998) [arXiv:hep-ex/9807003].

[5] Q. R. Ahmad *et al.* [SNO Collaboration], Phys. Rev. Lett. **87**, 071301 (2001) [arXiv:nucl-ex/0106015].

[6] J. Lesgourgues and S. Pastor, Phys. Rept. **429**, 307 (2006) [arXiv:astro-ph/0603494].

[7] A. Osipowicz *et al.* [KATRIN Collaboration], arXiv:hep-ex/0109033.

[8] S. R. Elliott and P. Vogel, Ann. Rev. Nucl. Part. Sci. **52**, 115 (2002) [arXiv:hep-ph/0202264].

[9] E. Komatsu *et al.* [WMAP Collaboration], Astrophys. J. Suppl. **192**, 18 (2011) [arXiv:1001.4538 [astro-ph.CO]].

[10] S. Tremaine and J. E. Gunn, Phys. Rev. Lett. **42**, 407 (1979).

[11] B. W. Lee and S. Weinberg, Phys. Rev. Lett. **39**, 165 (1977).

[12] A. D. Dolgov, S. H. Hansen, S. Pastor, S. T. Petcov, G. G. Raffelt and D. V. Semikoz, Nucl. Phys. B **632**, 363 (2002) [arXiv:hep-ph/0201287].

[13] G. Mangano, G. Miele, S. Pastor, T. Pinto, O. Pisanti and P. D. Serpico, Nucl. Phys. B **729**, 221 (2005) [arXiv:hep-ph/0506164].

[14] C. Quigg, arXiv:0802.0013 [hep-ph].

[15] C. P. Ma and E. Bertschinger, Astrophys. J. **455**, 7 (1995) [arXiv:astro-ph/9506072].

[16] P. de Bernardis *et al.* [Boomerang Collaboration], Nature **404**, 955 (2000) [arXiv:astro-ph/0004404].

[17] S. Hanany *et al.*, Astrophys. J. **545**, L5 (2000) [arXiv:astro-ph/0005123].

[18] C. L. Bennett *et al.* [WMAP Collaboration], Astrophys. J. Suppl. **148**, 1 (2003) [arXiv:astro-ph/0302207].

[19] Code for Anisotropies in the Microwave Background, available at http://camb.info/

[20] R. H. Brandenberger, arXiv:hep-ph/9210261.

[21] K. Ichikawa, T. Sekiguchi and T. Takahashi, Phys. Rev. D **78**, 083526 (2008) [arXiv:0803.0889 [astro-ph]].

[22] L. Pogosian, A. Silvestri, K. Koyama and G. B. Zhao, Phys. Rev. D **81**, 104023 (2010) [arXiv:1002.2382 [astro-ph.CO]].

[23] A. Silvestri and M. Trodden, Rept. Prog. Phys. **72**, 096901 (2009) [arXiv:0904.0024 [astro-ph.CO]].

[24] G. Danby, J-M. Gaillard, K. Goulianos, L. M. Lederman, N. Mistry, M. Schwartz and J. Steinberger, Phys. Rev. Lett. **9**, 36 (1962).

[25] S. Hannestad, H. Tu and Y. Y. Y. Wong, JCAP **0606**, 025 (2006) [arXiv:astro-ph/0603019].